Available online at www.sciencedirect.com
ScienceDirect
Journal of Catalysis 246 (2007) 382–389
JOURNAL OF CATALYSIS
www.elsevier.com/locate/jcat

Selective modification of surface and bulk V^{5+}/V^{4+} ratios and its effects on the catalytic performance of Mo–V–Te–O catalysts

Yihan Zhu [a], Weimin Lu [a,*], Han Li [a], Huilin Wan [b]

[a] *Institute of Catalysis, Zhejiang University (Xixi Campus), Hangzhou 310028, PR China*
[b] *Department of Chemistry and Institute of Physical Chemistry, Xiamen University, Xiamen 361005, PR China*

Received 17 October 2006; revised 21 December 2006; accepted 22 December 2006

Available online 2 February 2007

Abstract

Selective modification of surface and bulk V^{5+}/V^{4+} ratios in Mo–V–Te–O catalysts has been achieved using nitric acid and saturated ammonia solutions as pH adjustors. The addition of nitric acid strongly suppressed V^{4+} in the bulk but encouraged it on the surface. Because the bulk-phase compositions of Mo–V–Te–O catalysts varied only slightly, the changes in the catalytic performance for selective propane oxidation to acrolein resulted mainly from the variation of the bulk and surface V^{5+}/V^{4+} ratios. The high concentration of surface V^{5+} that was responsible for propane activation led to high selectivity of propylene and high conversion of propane. Increased bulk V^{4+} might result in oxygen vacancies, which promote the electron and oxygen transfer so as to increase the selectivity of deep oxidation products (CO_x). A low bulk V^{4+} concentration prefers selective oxidation products; the yield of acrolein was as high as 21.4%.

Keywords: Propane; Selective oxidation; V^{5+}/V^{4+} ratio; Acrolein; Mo–V–Te–O catalysts; Surface and bulk

1. Introduction

Propane is one of the most important constituents in natural gas and crude oil, but it has not been widely used up to now. In recent years, studies have focused mainly on one-step oxidation of propane to partial oxidation products via VPO [1,2] or MMO catalysts [3–7]. Acrolein (ACR) is a very important product that has wide applications in both the chemical and medical industries. Although the conventional catalytic process from propylene to acrolein shows a very high yield of acrolein [8–11], developing catalysts for the direct selective oxidation of propane to acrolein is needed for optimal use of this abundant resource.

Of all the catalysts studied, Mo–V–Te–(Nb)–O systems have proven effective for selective propane oxidation to acrolein or acrylic acid (AA) [5–7]. It is clear that the orthorhombic M1 phase (formulated as $(Te_2O)M_{20}O_{56}$, M = Mo, V, or Nb) functions mainly in the activation of propane [12]. The pseudo-hexagonal M2 phase [13] (formulated as $(TeO)M_3O_9$, M = Mo, V, or Nb) might act as an assistant phase and enhance the selectivity of acrylic acid [14].

Detailed studies on mechanisms of propane activation [15–18] have proved that, based on those phases, the abstraction of methylene-H as propane activation step occurs mainly at surface $^{5+}V{=}O$ sites. The surface $^{5+}V{=}O$ group might either generate a resonance form with a partial radical character for H abstraction [15] or process a typical 5 + 2 activation mechanism via dual M=O sites as advocated in VO_x/ZrO_2 catalysts [16], which are still under debate. A Te^{4+} site with a lone pair of electrons has been shown to be active for the α-H abstraction of the formed propylene, whereas a Mo^{6+} site is responsible for the chemisorption and O insertion of intermediate products to form oxygenated products [15]. Additive studies have showed that Mo^{6+}/Mo^{5+}, V^{5+}/V^{4+}, and Te^{6+}/Te^{4+} pairs always coexist on the surface and/or in the bulk of Mo–V–Te–(Nb)–O catalysts [19,20]. Those pairs might perform as follows: (i) Change the amounts of surface/bulk anion vacancies and promote electron and oxygen transfer (as Fe^{3+}/Fe^{2+} does in Mo-Bi catalysts [11]), (ii) generate different amounts of highly reactive surface

* Corresponding author. Fax: +86 571 88273283.
E-mail address: luweimin@zju.edu.cn (W. Lu).

0021-9517/$ – see front matter
doi:10.1016/j.jcat.2006.12.019

oxygen species (e.g., terminal M=O species), and (iii) serve as a bulk oxygen reservoir, avoiding the reconstruction of surface key structures during reaction [19]. The V^{5+}/V^{4+} pair has been shown to perform a dominant role in changing the catalytic activity of VPO catalysts for selective oxidation of *n*-butane [21]. It is difficult to make clear the function of each pair in the Mo–V–Te–O multielement systems, due to the difficulty of altering one pair while the others remain. Moreover, the different characters of such pairs on the surface and in the bulk have rarely been studied respectively, and no detailed relationship between the variation of such pairs and catalytic performance has been established.

In this paper, we used different pH adjustors for the preparation of Mo–V–Te–O catalysts. Both bulk and surface cases were studied, because they often shared quite different properties. Results showed that we succeeded in changing the relative amount of V^{5+}/V^{4+} pairs both on the surface and in the bulk rather than the Mo^{6+}/Mo^{5+} and Te^{6+}/Te^{4+} pairs for Mo–V–Te–O catalysts. With similar phase compositions, obvious changes in the performance of catalysts demonstrated the role of vanadium as a significant redox element and the important relationship between the V^{5+}/V^{4+} pair and catalytic performance.

2. Experimental

2.1. Catalyst preparation

All catalysts were prepared by an aqueous solution reaction method, using ammonium heptamolybdate (AHM) [$(NH_4)_6Mo_7O_{24}\cdot 4H_2O$], ammonium metavanadate (NH_4VO_3), and telluric acid (H_6TeO_6) as starting materials. They were dissolved in 20 ml of deionized water according to the corresponding composition at 353 K. For unitary system, the solutions were then used for the next step; three of the solutions were mixed together for ternary systems. The mixed solutions were adjusted to desired pH values with the adjusters of aqueous nitric acid (1.0 M) and ammonia (saturated solution). The original Mo–V–Te mixed solution exhibited a pH of 5.0 without the addition of any pH adjustors. Then the solutions were evaporated at 353 K to dryness and successively calcined at 873 K for 2 h in an N_2 stream.

2.2. Catalyst characterization

Powder X-ray diffraction (XRD) analysis was carried out using a Rigaku-D/Max-B automated powder X-ray diffractometer by the continuous scanning (4°/min from 3° to 80° of Bragg's angles 2θ) with Cu$K\alpha$ radiation ($\lambda = 0.15418$ nm) operating at 45 kV and 40 mA. Phase qualitative and reference intensity ratio (RIR) semiquantitative analyses were done using a MDI JADE v 6.5 software package.

Laser Raman spectra (LRS) were collected under ambient conditions using an HR LabRaman 800 system equipped with a CCD detector. A green laser beam ($\lambda = 514.5$ nm) was used for excitation.

Oxygen thermogravimetry/derivative thermogravimetry (O_2-TG/DTG) analysis was carried out in a Perkin–Elmer TGA7 thermogravimetric analyzer under pure oxygen atmosphere of 0.1 MPa and a ramp rate of 10 K/min. Data processing was done using a Pyris TGA7HT software package. BET specific surface area analysis of the catalysts was done using a Coulter Ominisorp 100CX automated gas sorption analyzer.

X-ray photoelectron spectroscopy (XPS) experiments were carried out on a RBD upgraded PHI-5000C ESCA system (Perkin–Elmer) with Mg$K\alpha$ radiation ($h\nu = 1253.6$ eV). The X-ray anode was run at 250 W, and the high voltage was kept at 14.0 kV, with detection angle at 54°. The base pressure of the analyzer chamber was about 5×10^{-8} Pa. The sample was directly pressed to a self-supported disk (10 × 10 mm) and mounted on a sample holder, then transferred into the analyzer chamber. Binding energies were calibrated using the contaminant carbon (C 1s = 284.5 eV). The data analysis was carried out using the RBD AugerScan 3.21 software provided by RBD Enterprises. The relative ratios of Mo^{6+}/Mo^{5+}, V^{5+}/V^{4+}, and Te^{6+}/Te^{4+} pairs were determined by smoothing and deconvolution of Mo 3d, V $2p_{3/2}$, and Te $3d_{5/2}$ peaks, respectively, with Gaussian curves. The background was subtracted using Shirley integrated function.

2.3. Catalytic activity test

Catalytic performance experiments were carried out in a fixed-bed quartz tubular reactor (6 mm i.d.; 200 mm long) under atmospheric pressure. Fresh 200-mg catalyst samples with similar volumes of catalyst bed were induced into the reactor under the feedstock of $O_2/C_3H_8 = 1.08/1$ (GHSV = 3000 h^{-1}). The reactants and products were analyzed using an on-line gas chromatograph equipped with Porapak Q (4.0 m × 1/8 in.) and TDX-01 carbon molecular sieve (2.0 m × 1/8 in.) columns. FID and TCD detectors were used for the two-channel detection of both columns. Catalytic reaction temperature varied from 623 to 773 K, and a blank experiment showed that homogeneous reaction can be neglected under our reaction conditions.

3. Results and discussion

3.1. Selective modification in unitary systems

As-synthesized MoO_x, VO_x, and TeO_x unitary catalysts were used to study the effects of pH adjustors on each of Mo^{6+}/Mo^{5+}, V^{5+}/V^{4+}, and Te^{6+}/Te^{4+} cation pairs, respectively. Powder XRD results showed that the unitary catalysts prepared under different pH values exhibited the presence of MoO_3 (JCPDS, 76-1003), Mo_4O_{11} (JCPDS, 72-0448), and Mo_9O_{26} (JCPDS, 73-1536) in MoO_x; V_6O_{13} (JCPDS, 71-2235), VO_2 (JCPDS, 76-0456), or V_2O_5 (JCPDS, 85-0601) in VO_x; and TeO_2 (JCPDS, 78-1713) in TeO_x. All phases were well crystallized, with no amorphous phases clearly observed, which made the further semiquantitative analysis (RIR method) more reliable. The results of the semiquantitative analysis for the unitary catalysts are given in Table 1. According to the phase proportion, we could simply calculate the average bulk

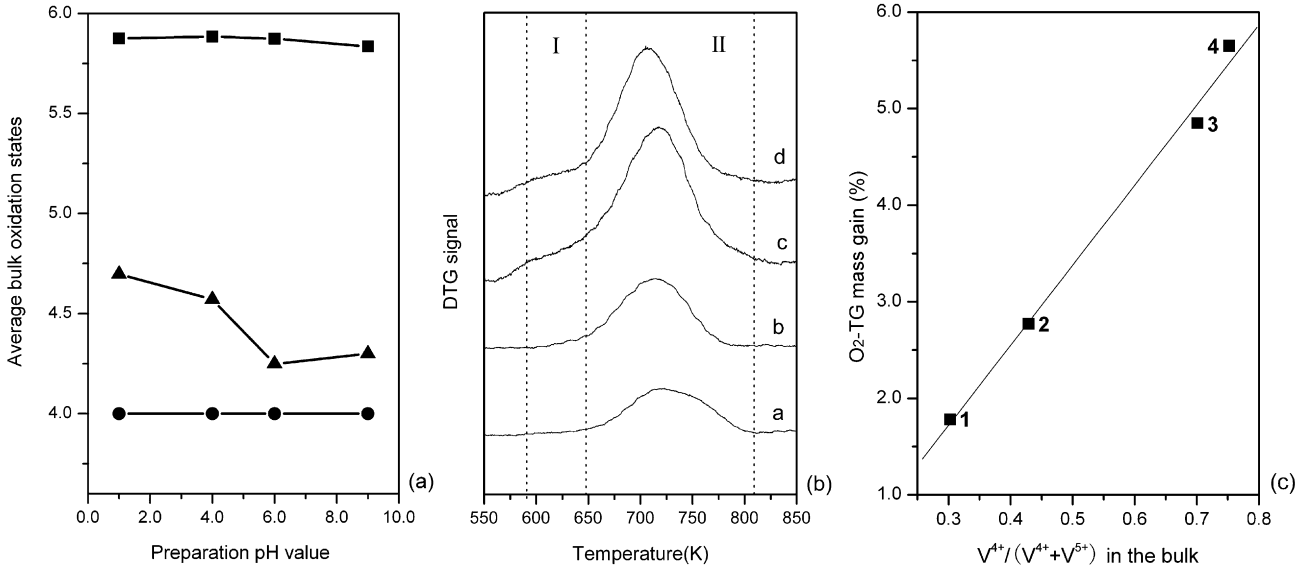

Fig. 1. (a) Average bulk oxidation states of the metal elements in MoO_x, VO_x, and TeO_x unitary catalysts versus different pH values. (●) TeO_x, (▲) VO_x, (■) MoO_x. (b) The O_2-DTG patterns of VO_x catalysts prepared under the pH of 1.0, 4.0, 6.0, and 9.0 with the curves from a to d, respectively. (c) Correlation between the O_2-TG mass gain and the bulk $V^{4+}/(V^{4+} + V^{5+})$ ratio for VO_x prepared under: dot 1, pH 1.0; dot 2, pH 4.0; dot 3, pH 9.0; dot 4, pH 6.0.

Table 1
Semi-quantitative phase analysis of as-synthesized MoO_x, VO_x, and TeO_x catalysts

Catalyst	pH value	Relative proportion of phases (wt%)		
MoO_x	1.0/4.0/6.0/9.0	MoO_3 65/69/67/58	Mo_4O_{11} 16/16/18/25	Mo_9O_{26} 19/15/15/17
VO_x	1.0/4.0/6.0/9.0	V_6O_{13} 39/63/75/90	VO_2 0/0/25/10	V_2O_5 61/37/0/0
TeO_x	1.0/4.0/6.0/9.0	TeO_2 100/100/100/100		

chemical states of each element as showed in Fig. 1a. It was obvious that the bulk chemical state of vanadium varied from 4.25 to 4.70 when the pH value changed from 9.0 to 1.0, which indicated that the addition of nitric acid strongly and selectively suppressed the formation of V^{4+} in the bulk. However, the bulk Mo^{6+}/Mo^{5+} and Te^{6+}/Te^{4+} ratios varied inappreciably. Actually, bulk Te^{4+} always remained unchanged, as suggested by the XRD results.

O_2-DTG experiments were carried out to verify the changes in the chemical state of the VO_x samples; the results are shown in Fig. 1b. Based on the phase composition achieved, the mass gain shoulders in region I (593–646 K) of Fig. 1b were due to the oxidation of V^{4+} in VO_2, because the shoulder in curve d of Fig. 1b became more intense when VO_2 increased in curve c and disappeared when no VO_2 existed in curves a and b. Similarly, the peaks at around 716 K in region II (646–810 K) might be attributed to the oxidation of V^{4+} in V_6O_{13} according to the XRD semiquantitative results. Fig. 1c shows good linear correlation between the bulk $V^{4+}/(V^{4+} + V^{5+})$ ratio and O_2-TG mass gain. It was practical to reflect the bulk amount of V^{4+} by the O_2-TG mass gains. This point would be further used in the Mo–V–Te–O ternary catalysts. Single broad mass gain peak around 751 K ranged from 677 to 850 K appeared in MoO_x catalysts, and no oxygen consumption peak occurred in TeO_x catalysts (O_2-DTG patterns of MoO_x and TeO_x catalysts not shown here).

The mass gain shoulders of VO_2 generally appeared at lower temperatures than those of V_6O_{13}, indicating that V^{4+} in VO_2 was more reducible than in V_6O_{13}. In conclusion, the addition of nitric acid suppressed the existence of V^{4+}, but had little effect on the Mo^{6+}/Mo^{5+} and Te^{6+}/Te^{4+} ratios in the bulk, in accordance with the results of powder XRD.

3.2. Selective modification in $MoV_{0.3}Te_{0.25}O_x$ mixed catalysts

3.2.1. Bulk studies of the modifications

The Mo–V–Te–O ternary catalysts under different pH values were prepared with the composition of $MoV_{0.3}Te_{0.25}O_x$. Freshly prepared catalysts were all black powders with very small specific surface area, as suggested by BET experiments ($<1.0\ m^2/g$).

According to the powder XRD results, $MoV_{0.3}Te_{0.25}O_x$ catalysts were generally composed of orthorhombic $TeMo_5O_{16}$ phase (JCPDS, 80-1238) with $2\theta = 8.8°$, 13.0°, 17.7°, 21.8°, 26.2°, 26.7°, 30.5°, 37.8°, and 48.4° and pseudohexagonal M2 phase (TeM_3O_{10}, M = Mo or V [22]) with peaks at 14.0°, 22.1°, 23.2°, 25.3°, 26.3°, 28.2°, 33.1°, 36.1°, and 45.3° [13,23]. The absence of low-angle peaks at 6.6°, 7.8°, and 9.0° in all $MoV_{0.3}Te_{0.25}O_x$ catalysts implies that no M1 structured phase existed [13], though M1 phase sometimes coexisted with M2 phase as in the Mo–V–Te–Nb–O catalyst system [22–25]. Comparison of peak areas at 30.5° for orthorhombic $TeMo_5O_{16}$ phase and 36.1° for M2 phase was used for calculating their relative quantities in a semiquantitative view, because these two peaks did not overlap with other diffraction peaks. XRD patterns and phase composition are shown in Fig. 2. The results clearly show that the catalysts prepared under pH 1.0 and 5.0 had similar phase composition and that the $TeMo_5O_{16}$ phase increased slightly in the catalyst prepared

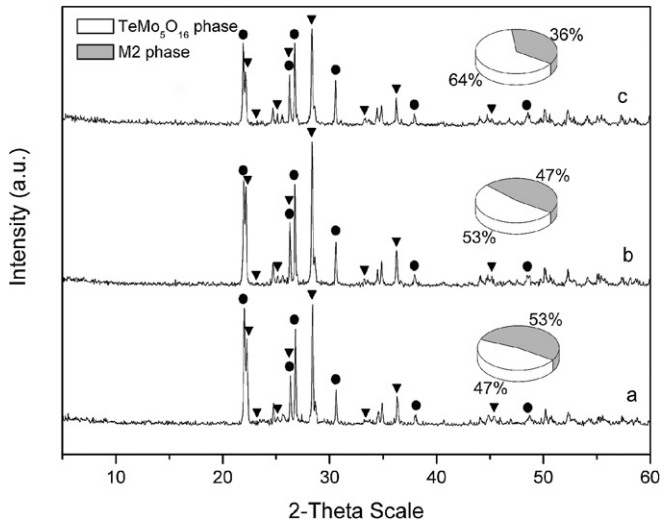

Fig. 2. Powder XRD patterns of the $MoV_{0.3}Te_{0.25}O_x$ catalysts prepared under the pH of (a) 1.0, (b) 5.0, and (c) 9.0. And relative quantity of $TeMo_5O_{16}$ and M2 phases derived by semi-quantitative analysis. (●) $TeMo_5O_{16}$ phase, (▼) M2 phase.

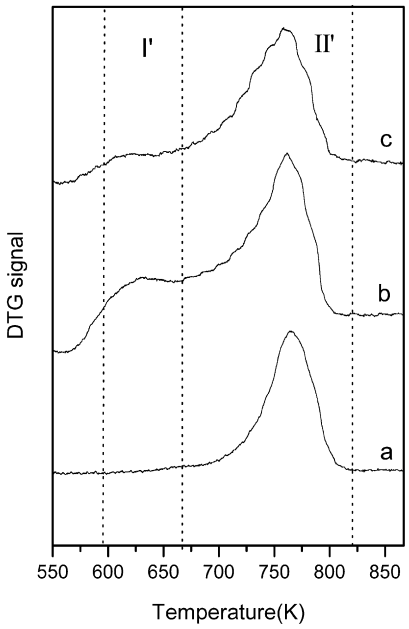

Fig. 3. O_2-DTG patterns of the $MoV_{0.3}Te_{0.25}O_x$ catalysts prepared under the pH of (a) 1.0, (b) 5.0, and (c) 9.0.

under pH 9.0. All of the phases were also well crystallized, as suggested in the XRD patterns.

O_2-DTG experiments (Fig. 3) of the Mo–V–Te–O catalysts showed the changes in the chemical states of elements in the bulk. The shoulders in region I′ (596–673 K) could be attributed to the oxidation of V^{4+} to stable V^{5+} in the V-containing M2 phase, as it was within a similar oxidation temperature region with V^{4+} in VO_2. The main peak at 755 K in region II′ (above 673 K) might be attributed to the oxidation of Mo^{5+} to Mo^{6+}, because the peak situated at similar temperature region as in the MoO_x catalysts. The intensity of the peak in region II′ varied inappreciably. Considering that Te^{4+} exists only in TeO_x catalysts, and based on the numerous related studies on the bulk mixed Mo–V–Te–(Nb)–O systems [19,20], bulk Te^{4+} was thought to be stably formed in $MoV_{0.3}Te_{0.25}O_x$ catalysts.

It was observed that shoulders in region I′ decreased in Fig. 3c and disappeared in Fig. 3a. These results demonstrate that the addition of nitric acid strongly suppressed the amount of bulk V^{4+} in Mo–V–Te–O catalysts, and the addition of ammonia also suppressed bulk V^{4+} to a lesser extent. This effect was less obvious with Mo^{6+}/Mo^{5+} pairs. Because the catalysts prepared under pH 1.0 and 5.0 had similar phase composition, the variation of V^{5+}/V^{4+} ratio took place in the V-containing M2 phase rather than in the $TeMo_5O_{16}$ phase. Thus, the M2 phase exhibited oxygen nonstoichiometry preferentially controlled by the bulk V^{5+}/V^{4+} ratio. When V^{4+} substitutes for V^{5+} in the bulk, some oxygen vacancies could be induced. Because the mass gain shoulders of V^{4+} were in lower temperature ranges, those V^{4+} sites might exhibit strong reducibility and tend to be oxidized by oxygen species under reaction conditions. Therefore, the bulk V^{4+} plays a significant role in promoting electron and oxygen transfer during reaction.

3.2.2. *Surface studies of the modifications*

XPS experiments were used to detect the surface modifications after addition of pH adjustors. The surface composition seemed to be different, as shown in Table 2, possibly due to segregation. Furthermore, the surface concentration of vanadium increased slightly when nitric acid was added into Mo–V–Te mixed solutions.

The results of peak fitting in XPS are shown in Fig. 4 and Table 2. For the deconvolution of Mo 3d core level, a splitting energy of about 3.15 eV with the intensity ratio of $I(3d_{5/2}):I(3d_{3/2}) = 3/2$ for each Mo $3d_{5/2}$–Mo $3d_{3/2}$ doublet was used [26]. Consequently, the peaks with BE of 235.3 ∼235.6 eV were attributed to Mo^{6+} $3d_{3/2}$, together with another weak line around 234.5 eV for Mo^{5+} $3d_{3/2}$ [19,26–28]. The two lines showed an energy shift around 0.9 eV [19,20]. Similarly, the Mo^{6+} $3d_{5/2}$ was at 232.4 eV and Mo^{5+} $3d_{5/2}$ was at 231.3–231.5 eV. The $Mo^{5+}/(Mo^{5+} + Mo^{6+})$ ratio was calculated via the fitted peak areas and showed that surface Mo^{5+} decreased slightly when nitric acid was induced.

The extremely sharp changes in V $2p_{3/2}$ core level reflected that the surface modification was also selective for vanadium. The curve-fitting results showed that the main peaks could be deconvoluted into two lines at around 517.1 and 516.2 eV, which could be assigned to the presence of surface V^{5+} and V^{4+}, respectively [29,30]. From Fig. 4, the surface V^{5+} of Mo–V–Te–O catalysts was strongly suppressed when nitric acid was induced (curve a), opposite to the situation in the bulk. The addition of ammonia could also decrease surface V^{5+} species.

The deconvolution of Te $3d_{5/2}$ peaks showed that all of the peaks can be fitted into two components. The line with BE of 576.9 eV was assigned to Te^{6+} $3d_{5/2}$, and the line at 575.9 eV was attributed to Te^{4+} $3d_{5/2}$ (reported BEs of Te^{6+} $3d_{5/2}$ and Te^{4+} $3d_{5/2}$ were 576.6 and 575.7 eV, respectively) [31]. The presence of both Te^{6+} and Te^{4+} on the surface was in accordance with results reported earlier [32]. The results of XPS characterization showed that the addition of nitric acid and ammonia as pH adjustors slightly changed the relative amount

Table 2
Surface compositions, surface Mo^{6+}/Mo^{5+}, V^{5+}/V^{4+}, and Te^{6+}/Te^{4+} ratios by XPS, and I_{992}/I_{963} ratio by Raman spectroscopy

Samples	Surface composition	$V^{5+}/(V^{5+}+V^{4+})$	$Mo^{5+}/(Mo^{5+}+Mo^{6+})$	$Te^{6+}/(Te^{6+}+Te^{4+})$	I_{992}/I_{963}
pH 1.0	$MoV_{0.28}Te_{0.26}O_{4.05}$	0.00	0.00	0.44	0.07
pH 5.0	$MoV_{0.24}Te_{0.32}O_{4.19}$	0.53	0.02	0.50	2.71
pH 9.0	$MoV_{0.22}Te_{0.23}O_{3.78}$	0.44	0.06	0.51	0.74

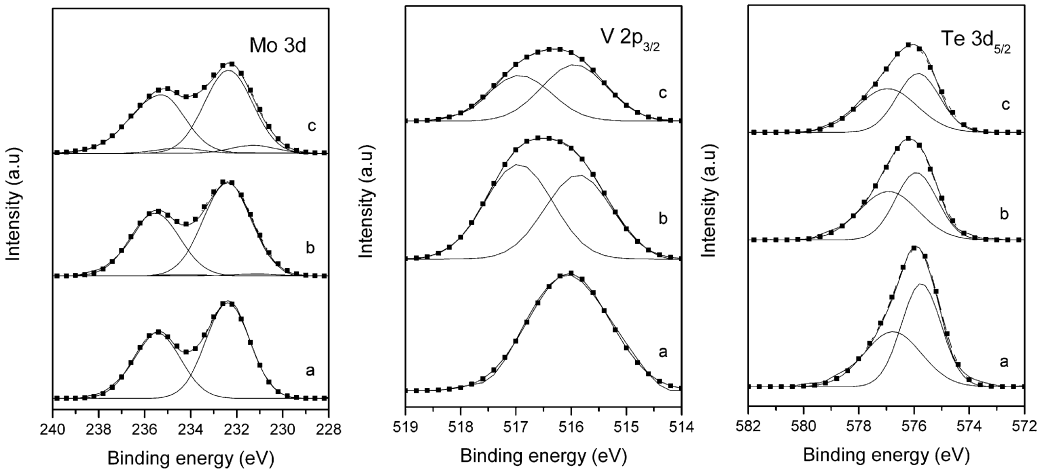

Fig. 4. XPS spectrum of Mo 3d, V $2p_{3/2}$, and Te $3d_{5/2}$, and their deconvolution results. (a) pH 1.0, (b) pH 5.0, and (c) pH 9.0.

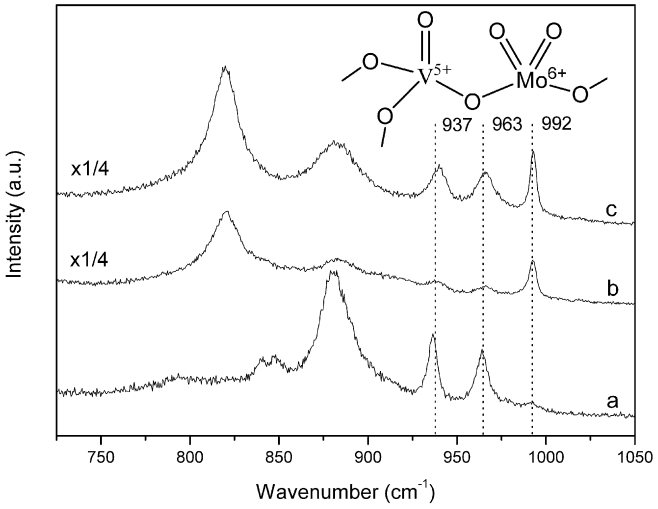

Fig. 5. Raman spectra of the $MoV_{0.3}Te_{0.25}O_x$ catalysts under pH value of (a) 1.0, (b) 5.0, and (c) 9.0.

of Te^{6+}. Surface Te^{6+} and Te^{4+} species were in almost equal amounts, accounting for the existence of oxygen reservoirs for the α-H abstraction of propylene and allylic species as intermediate products [19].

Raman spectra of the $MoV_{0.3}Te_{0.25}O_x$ catalysts are shown in Fig. 5. The peaks above 900 cm^{-1} were generally attributed to the stretch mode of terminal M=O (M = Mo or V) species [33]. In detail, the band at 992 cm^{-1} suggested the presence of terminal V=O [34,35], and bands at 963 and 937 cm^{-1} could be due to typical Mo=O species [36,37]. The relative surface V=O concentration was evaluated by calculating the intensity ratios of the bands at 992 and 963 cm^{-1} (I_{992}/I_{963}) in Table 2. For the catalyst prepared under pH 5.0, the I_{992}/I_{963} ratio reached a maximum of 2.71 and dropped to a minimum for the catalyst when pH 1.0. Combined with the XPS results, this indicates that the surface concentration of V^{5+} increased when V=O increased; thus, the enhanced surface V^{5+} should be present in the terminal $^{5+}V{=}O$ form.

3.3. Catalytic performance of $MoV_{0.3}Te_{0.25}O_x$ catalysts

The reaction results of selective oxidation from propane to acrolein on $MoV_{0.3}Te_{0.25}O_x$ catalysts are shown in Table 3. Carbon oxides, propylene, acrolein, acetic acid, acrylic acid, formaldehyde, acetaldehyde, ethylene, methane, and acetone were detected as products.

The addition of pH adjustors strongly affected the performance of the Mo–V–Te–O catalysts. Compared with the reaction results of pH 5.0, the selectivity of ACR increased greatly (from 20.5 to 48.4%), and the selectivity of CO_x decreased significantly, although the conversion of propane was also decreased at pH 1.0. At pH 9.0, the conversion of propane was nearly the same as that at pH 5.0, and selectivity of ACR augmented in some sort.

The $MoV_{0.3}Te_{0.25}O_x$ catalysts prepared under 1.0 and pH 5.0 had similar phase composition. Moreover, only the V^{5+}/V^{4+} pair was selectively modified in the catalysts. The obvious changes in catalytic performance were due mainly to the variation of surface and bulk V^{5+}/V^{4+} ratios. It indicated that vanadium acted as a redox element in both surface and bulk.

The relationship between the selectivity of oxidation products and O_2-TG mass gain in region I′ is shown in Fig. 6a. When bulk V^{4+} increased, the conversion of propane and selectivity of CO_x rose. In contrast, the selectivity of (ACR + AA) as selective oxidation products decreased. Table 3 also shows that the

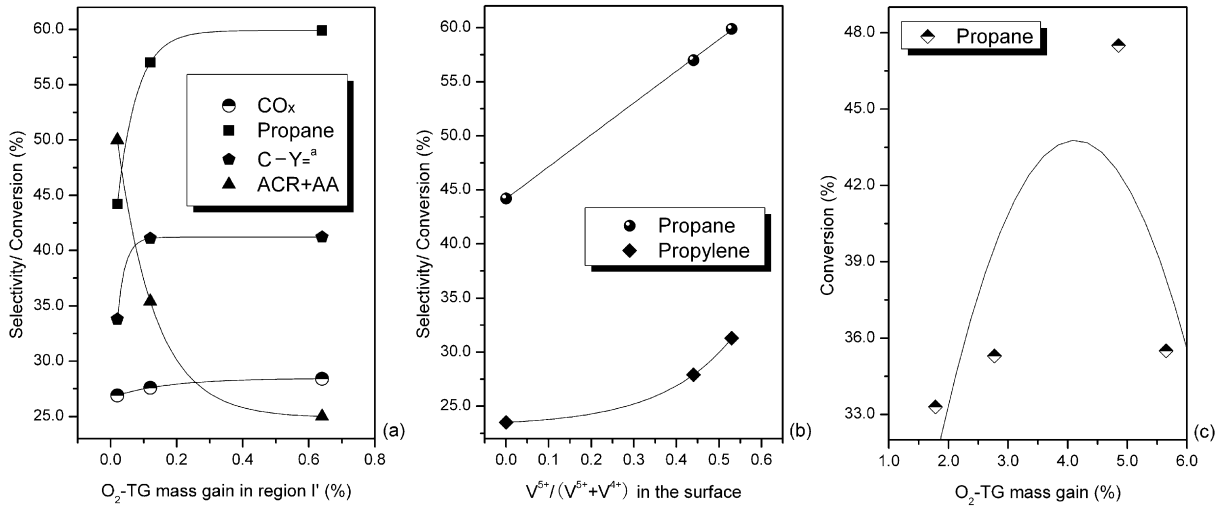

Fig. 6. Correlation between selectivity of products/conversion of propane (a) and the O_2-TG mass gain in region I′, (b) and the surface $V^{5+}/(V^{5+} + V^{4+})$ ratio in $MoV_{0.3}Te_{0.25}O_x$ catalysts. (c) Relationship between conversion of propane and the O_2-TG mass gain in VO_x. [a] Conversion of propane minus the yield of propylene.

Table 3
Catalytic performance on VO_x and $MoV_{0.3}Te_{0.25}O_x$ catalysts prepared under different pH values[a]

Catalysts	pH	Conversion of propane (%)	Selectivity of products (%)								Yield of ACR (%)
			CO	CO_2	ACR[b]	AA[b]	AcA[b]	Alde[b]	C_3H_6	Others[b]	
$MoV_{0.3}Te_{0.25}O_x$	1.0	44.2	13.5	3.4	48.4	0.6	3.6	5.1	23.5	1.9	21.4
	5.0	59.9	21.8	6.6	20.5	4.5	3.5	4.4	31.3	7.4	12.3
	9.0	57.0	20.4	7.2	27.6	7.8	2.6	1.7	27.9	4.8	15.7

[a] Temperature: 773 K, feedstock: $O_2/C_3H_8 = 1.08/1$, GHSV: 3000 h^{-1}.
[b] ACR: acrolein, AA: acrylic acid, AcA: acetic acid, Alde: formaldehyde and acetaldehyde, Others: acetone, ethylene, and methane, etc.

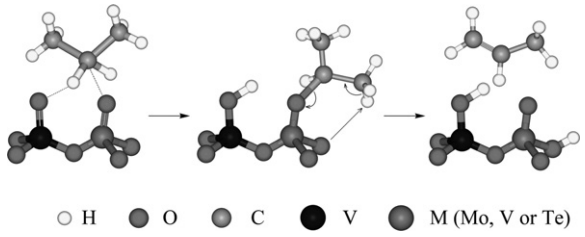

Fig. 7. 5 + 2 pathway of propane activation forming propylene by surface $^{5+}V{=}O$ and M=O (M = Mo, V or Te) dual sites.

selectivity of AA increased compared with that of ACR at increasing pH values. Because AA is the consecutive O-inserting product of ACR, the catalysts having more bulk V^{4+} at pH 5.0 or 9.0 were also prone to further oxidation of ACR.

As stated earlier, the oxygen vacancies ($V_O^{\bullet\bullet}$) formed by the bulk V^{4+} (V'_V) could be oxidized by dioxygen, with bulk lattice oxygen species ($O_{O(BL)}$) produced. The bulk lattice oxygen species might oxidize the other active sites (M'_M) reduced by reactants and intermediate products on the surface, thus producing surface lattice oxygen species ($O_{O(SL)}$). The process using Kröger–Vink notations is as follows:

$$2V'_{V(B)} + V_{O(B)}^{\bullet\bullet} + \frac{1}{2}O_2(g) \rightarrow 2V_{V(B)} + O_{O(BL)}, \quad (1)$$

$$2V_{V(B)} + O_{O(BL)} + 2M'_{M(S)} + V_{O(S)}^{\bullet\bullet} \rightarrow 2V'_{V(B)} + O_{O(SL)} + 2M_{M(S)} + V_{O(B)}^{\bullet\bullet}. \quad (2)$$

The more bulk V^{4+} in the catalyst, the more oxygen vacancies produced, and the easier the transfer of electron and oxygen species. Because their mobilities were enhanced, the reactant and intermediate species adsorbed on the active sites would have increased potential for attack by electrophilic oxygen species. As a result, the activation of propane became more facile, and the intermediate products tended to be overoxidized. This indicates that specific bulk V^{4+}/V^{5+} ratio might offer the best cooperation between electron and oxygen transfer and propane activation rate and achieve the highest propane conversion. The correlation between the amount of bulk V^{4+} (in terms of O_2-TG mass gain in region I′, as shown in Fig. 6c) and conversion of propane in VO_x catalysts illuminated this point. When the bulk V^{4+}/V^{5+} ratio reached 4.85, a maximum propane conversion of 47.5% was achieved.

On the other hand, surface V^{5+} in the $^{5+}V{=}O$ form also provided significant effects on the catalytic performance as Fig. 6b shows. As surface $V^{5+}/(V^{5+} + V^{4+})$ ratio increased from 0 to 0.53, the conversion of propane rose linearly from 44.2 to 59.9%. Because propylene was the intermediate product of the propane activation, propylene selectivity also increased from 23.5 to 31.3% as surface V^{5+} was enhanced. This confirms that the surface $^{5+}V{=}O$ groups play an important role in promoting propane activation and dehydrogenation. We considered a 5 + 2 pathway to be possible [16,17] as shown in Fig. 7.

It was necessary to eliminate the contribution of surface $^{5+}V{=}O$ to the conversion of propane to make the contribution

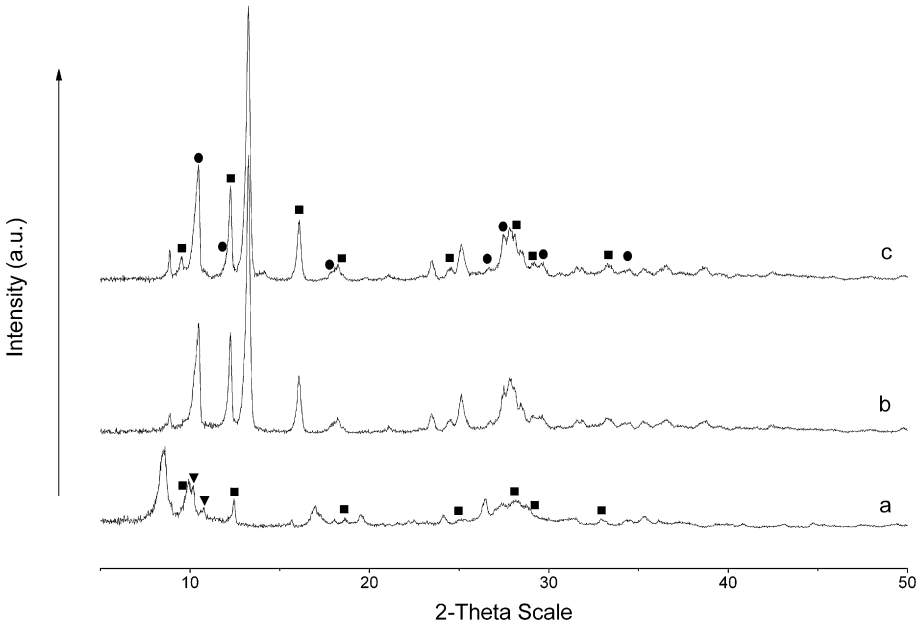

Fig. 8. Powder XRD patterns of the $MoV_{0.3}Te_{0.25}O_x$ precursors under pH value of (a) 1.0, (b) 5.0, and (c) 9.0. Phases marked as (●) $(NH_4)_6(TeMo_6O_{24})\cdot 7H_2O$, (■) $(NH_4)_2Mo_4O_{13}$, (▼) $(NH_4)_6V_{10}O_{28}\cdot 6H_2O$.

of bulk V^{4+} more clear. Because the propane conversion (C) minus the yield of propylene ($Y_=$) equals the total yield of all other oxidation products, curve $C–Y_=$ in Fig. 6a was used to represent the ability of further oxidation of the catalysts. The results show that the promotion of electron and oxygen transfer caused by more bulk V^{4+} was also advantageous to the further oxidation of intermediate products and increased propane conversion.

3.4. Preliminary study of the reason for selective modification

Interestingly, the addition of nitric acid and ammonia as pH adjustors could change the ratios of V^{5+}/V^{4+} pairs both in the bulk and on the surface. The precursors of the $MoV_{0.3}Te_{0.25}O_x$ ternary catalysts before heat treatment were characterized by powder XRD, as shown in Fig. 8.

XRD results showed that the precursors under pH 5.0 and 9.0 had similar compositions: $(NH_4)_2Mo_4O_{13}$ (JCPDS, 80-0757), $(NH_4)_6(TeMo_6O_{24})\cdot 7H_2O$ (JCPDS, 26-0080), and some unknown phases. However, the precursor prepared under pH 1.0 appeared to have quite different phase composition from the above two cases. $(NH_4)_2Mo_4O_{13}$, $(NH_4)_6V_{10}O_{28}\cdot 6H_2O$ (JCPDS, 82-0481), and some unknown phases were detected. $(NH_4)_6[TeMo_6O_{24}]\cdot 7H_2O$ has been shown to be the precursor of monoclinic $TeMo_5O_{16}$ [38], the structure of which has some relationship with the orthorhombic form of the $TeMo_5O_{16}$ phase. No known phase was recognized as the precursor of the M2 phase, and the $(NH_4)_6V_{10}O_{28}\cdot 6H_2O$ phase in the precursor did not significantly affect the phase composition of the catalysts under pH 1.0 and 5.0. Thus, different V^{5+}/V^{4+} ratios both in the bulk and on the surface of the catalysts prepared under different pH values were closely related to the unknown phases in the precursors. We think that the V-containing M2 phase might be yielded via a solid-state reaction (SSR) during heat treatment of the precursors. The reason for the inverse trend of changes in the V^{5+}/V^{4+} ratio between the bulk and surface remains under study.

4. Conclusions

As is well known, it is of great importance to add redox elements (e.g., V, Fe, Cr, Ce, Sn, U) into bicomponent catalysts to achieve better catalytic performance. Such redox elements exhibit higher redox potential than the inserting O species [15] and present mainly as V^{5+}/V^{4+}, Fe^{3+}/Fe^{2+}, Cr^{6+}/Cr^{5+}, Ce^{4+}/Ce^{3+}, Sn^{4+}/Sn^{2+}, and U^{6+}/U^{4+} pairs, possibly facilitating electron and oxygen transfer [11].

In generally, the addition of pH adjustors (HNO_3 or NH_3 solution) during preparation strongly affected the bulk and surface characteristics and catalytic properties of the Mo–V–Te–O catalysts. The modifications were always rather selective for vanadium as a vital redox element and preferentially changed the bulk and surface V^{5+}/V^{4+} ratios.

O_2-TG/DTG and XPS experiments revealed that bulk V^{4+} or surface V^{5+} in Mo–V–Te–O catalysts can be preferentially suppressed by addition of pH adjustors. The surface V^{5+} occurred in the $^{5+}V{=}O$ form. The bulk V^{4+} might play a significant role in promoting electron and oxygen transfer during reaction. Moreover, the oxygen nonstoichiometry of the M2 phase might result from the variable bulk V^{5+}/V^{4+} ratios balanced by oxygen vacancies. The M2 phase could possibly be described as $(TeO)M_3O_{9-\delta}$.

The activation of propane is closely related to the surface V^{5+} concentration, because the surface vanadyl group has proven rather active. The conversion of propane depends mainly on the surface $^{5+}V{=}O$ groups. On the other hand, higher bulk V^{4+} concentrations are related to more overoxidation products (CO_x), because bulk V^{5+}/V^{4+} pairs are responsible for electron

and oxygen transfer. Less bulk V^{4+} results in high selectivity of ACR as the selective oxidation product in Mo–V–Te–O catalysts. Consequently, optimum surface and bulk V^{5+}/V^{4+} ratios may be possible to achieve higher ACR yields.

Acknowledgment

This work was supported by the National Natural Science Foundation of China (grant 20473071).

References

[1] G. Landi, L. Lisi, J.C. Volta, Chem. Commun. (2003) 492.
[2] G. Landi, L. Lisi, J.C. Volta, J. Mol. Catal. A 222 (2004) 175.
[3] A. Kaddouri, C. Mazzocchia, E. Tempesti, Appl. Catal. A 180 (1999) 271.
[4] H. Jiang, W. Lu, H. Wan, J. Mol. Catal. A 208 (2004) 213.
[5] L. Chen, J. Liang, H. Lin, W. Weng, H. Wan, J.C. Védrine, Appl. Catal. A 293 (2005) 49.
[6] T. Ushikubo, Y. Koyasu, H. Nakamura, JP10045664 (1998).
[7] T. Ushikubo, K. Oshima, A. Kayou, M. Vaarkamp, M. Hatano, J. Catal. 169 (1997) 394.
[8] P. Botella, J.M. López Nieto, B. Solsona, J. Mol. Catal. A 184 (2002) 335.
[9] W. Gerhartz, Ullmann's Encyclopedia of Industrial Chemistry, VCH, Weinheim, 1985.
[10] G. Creten, D.S. Lafyatis, G.F. Froment, J. Catal. 154 (1995) 151.
[11] J.M.M. Millet, H. Ponceblanc, G. Coudurier, J.M. Herrmann, J.C. Védrine, J. Catal. 142 (1993) 381.
[12] M. Baca, A. Pigamo, J.L. Dubois, J.M.M. Millet, Top. Catal. 23 (2003) 39.
[13] P. DeSanto Jr., D.J. Buttrey, R.K. Grasselli, C.G. Lugmair, A.F. Volpe, B.H. Toby, T. Vogt, Z. Kristallogr. 219 (2004) 152.
[14] M. Baca, M. Aouine, J.L. Dubois, J.M.M. Millet, J. Catal. 233 (2005) 234.
[15] R.K. Grasselli, J.D. Burrington, D.J. Buttrey, P. DeSanto Jr., C.G. Lugmair, A.F. Volpe Jr., T. Weingand, Top. Catal. 23 (2003) 5.
[16] F. Gilardoni, A.T. Bell, A. Chakraborty, P. Boulet, J. Phys. Chem. B 104 (2000) 12,250.
[17] K.D. Chen, E. Iglesia, A.T. Bell, J. Phys. Chem. B 105 (2001) 646.
[18] G. Fu, X. Xu, X. Lu, H. Wan, J. Phys. Chem. B 109 (2005) 6416.
[19] M. Baca, J.M.M. Millet, Appl. Catal. A 279 (2005) 67.
[20] J.M.M. Millet, H. Roussel, A. Pigamo, J.L. Dubois, J.C. Jumas, Appl. Catal. A 232 (2002) 77.
[21] M.T. Sananes-Schulz, A. Tuel, G.J. Hutchings, J.C. Volta, J. Catal. 166 (1997) 388.
[22] M. Aouine, J.L. Dubois, J.M.M. Millet, Chem. Commun. (2001) 1180.
[23] T. Ushikubo, K. Oshima, A. Kayou, M. Hatano, Stud. Surf. Sci. Catal. 112 (1997) 473.
[24] B. Zhu, H. Li, W. Yang, L. Lin, Catal. Today 93–95 (2004) 229.
[25] B. Solsona, J.M. López Nieto, J.M. Oliver, J.P. Gumbau, Catal. Today 91–92 (2004) 247.
[26] G.-T. Kim, T.-K. Park, H. Chung, Y.-T. Kim, M.-H. Kwon, J.-G. Choi, Appl. Surf. Sci. 152 (1999) 35.
[27] J.-G. Choi, L.T. Thompson, Appl. Surf. Sci. 93 (1996) 143.
[28] K. Uchida, A. Ayame, Surf. Sci. 357–358 (1996) 170.
[29] G. Silversmit, D. Depla, H. Poelman, G.B. Marin, R. De Gryse, J. Electron. Spectrosc. Relat. Phenom. 135 (2004) 167.
[30] M. Demeter, M. Neumann, W. Reichelt, Surf. Sci. 41 (2000) 454.
[31] V.V. Guliants, R. Bhandari, J. Phys. Chem. B 109 (2005) 10,234.
[32] P. Botella, P. Concepción, J.M. López Nieto, Y. Moreno, Catal. Today 99 (2005) 51.
[33] G. Mestl, Catal. Rev. 40 (4) (1998) 451.
[34] J.H. Clark, The Chemistry of Titanium and Vanadium, Elsevier, New York, 1968.
[35] W. Chem, L. Mai, J. Peng, Q. Xu, Q. Zhu, J. Solid State Chem. 177 (2004) 377.
[36] I. Lindqvist, Ark. Kemi 2 (1951) 349.
[37] A.W. Armour, M.G.B. Dreu, P.C.H. Mitchell, J. Chem. Soc. Dalton Trans. 1975 (1975) 1493.
[38] I.L. Botto, C.I. Cabello, H.J. Thomas, Mater. Chem. Phys. 47 (1997) 37.